



Defense Technical Information Center Compilation Part Notice

This paper is a part of the following report:

- *Title:* Technology Showcase: Integrated Monitoring, Diagnostics and Failure Prevention.
Proceedings of a Joint Conference, Mobile, Alabama, April 22-26, 1996.

- *To order the complete compilation report, use:* AD-A325 558

The component part is provided here to allow users access to individually authored sections of proceedings, annals, symposia, etc. However, the component should be considered within the context of the overall compilation report and not as a stand-alone technical report.

Distribution Statement A:

This document has been approved for public release and sale; its distribution is unlimited.

19971126 018

DTIC
Information For The Defense Community

MULTISENSOR MONITORING OF GEAR TOOTH FATIGUE FOR PREDICTIVE DIAGNOSTICS

Grant A. Gordon, Amulya K. Garga, and Clark Moose
The Pennsylvania State University
Applied Research Laboratory
PO Box 30
State College, PA 16804 USA
gag100@psu.edu

Abstract: Successful machine diagnostics is critically dependent on the collection and processing of prognostic features that relate back to failure precursors. Since the significance of gear tooth failure is recognized as a critical component to the overall condition of drive train mechanical systems, single gear tooth failure has been examined. By employing a special jig to orient and constrain the gear samples, Hertzian loading was applied along a single contact line on the gear tooth to simulate the conditions seen during operation. Optical, ultrasonic and mechanical sensors measured a variety of observables including load, deflection, and acoustic emission. After monitoring the fatigue test with these three noncommensurate sensors, features of the data could consistently be related to crack growth phenomena. Data collection, analysis, and interpretation are discussed for spur gear samples that show both the absence and presence of cracks and support the validity of the extracted features as failure precursors. Cyclostationary analysis, an advanced signal processing techniques, was used to promote earlier indication and sharper resolution of these measures. The results demonstrate the potential for using nontraditional sensors and techniques, which are more amenable to commercial use, for an in situ monitoring system.

Key Words: Multisensor monitoring; condition based maintenance; cyclostationary; acoustic emission; gear tooth fatigue

INTRODUCTION: The ability to predict the remaining lifetime of a mechanical system is an area that, although is not presently realized, commands considerable attention from both commercial and military organizations. Effective machinery prognostic systems hold the promise of being able to reduce maintenance costs, improve safety margins, increase mission readiness and reduce waste through implementation of retirement for cause maintenance programs. Critical to this objective is the ability to estimate the time required for fault initiation and to track the progression of these failure precursors. Since even modern manufacturing methods can not create truly flawless materials, the notion of flaw initiation is one of semantics. Flaws are incipient within in the material, so effectively our objectives should be to detect, identify and track the progression of flaws with increased accuracy. Therefore, it is generally accepted [e.g. 1] that improvements in the prediction of remaining service life of a component will depend on this ability.

Traditionally the prediction of remaining lifetime has been done on a statistical basis. Large population databases are used to establish relationships between operating parameters and mechanical endurance. Because of their statistical nature however, the results of these studies are not directly applicable to an individual part or component. This fact is generally overlooked or mitigated by ensuring that significant safety 'margins' are applied before the data is employed in a maintenance regimen. This approach results in potentially large amounts of waste, since parts are replaced based on a conservative statistical estimate of lifetime rather than a more direct measure. There is also the potential that a failure will occur before the statistically predicted lifetime, which motivates the need for more accurate condition monitoring from the perspective of safety. In this paper we investigate techniques that can detect and track failure precursors in individual components rather than populations of parts. These features could potentially be used to develop a robust prognostic model that predicts the remaining useful life of the system by employing data fusion and intelligent reasoning techniques [2].

EXPERIMENTAL: As faults grow from micromechanical initiation sites and gain dominance over other potential failure sources, they manifest themselves in a number of ways throughout the system. This redundancy of information about the physical failure process suggests that different measures or perspectives can be combined to establish a more robust description of the underlying system. Furthermore, we expect that certain measures, or our ability to probe them, will be more sensitive to early fault detection while others will display attributes such as improved source identification.

In this paper we employed three sensing methods: acoustic emission, mechanical deflection and load measurements, and optical deflection measurements, to monitor the fatigue crack growth in a set of typical aircraft drive train gears. The gears were 32-tooth spur gears made from commercially accepted hardened steel. After the gears were modified by cutting alternating

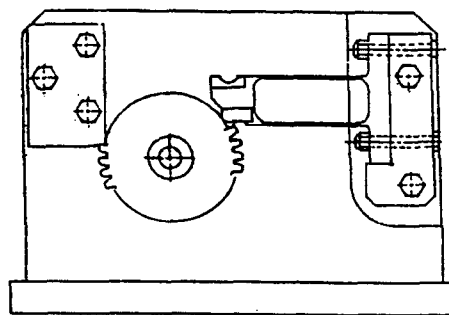


Figure 1. Gear fatigue test fixture

groups of four teeth from the periphery of the gear, they were placed in a test fixture (Figure 1) based on a Boeing gear fatigue apparatus [3]. This test fixture constrains the tooth loading along a line of contact at the highest point of single tooth contact. A Materials Testing System (MTS) cyclically drove the load frame ram onto the compliant armature of the fixture in a stress controlled manner. After an initial ramp up to the maximum load condition, the ram cycled at a rate of 20 Hz, Figure 2, between a minimum compressive load of 900 lb. and a maximum compressive load of 10,000 lb. Load and position data were collected from the MTS sensor head at rate of 100 samples per sec until the axial position of the loading head exceeded a preset deflection limit. This limit, which established the end of the testing sequence, was set at an 0.002 in. increase beyond the initial maximum deflection established at the onset of loading. Commensurate with this data collection, acoustic emission and optical data were collected with sensors that were triggered and synchronized with the MTS loading frame.

OPTICAL MEASUREMENTS: The optical setup used to measure deflection, was based on a knife edge detection arrangement, Figure 3. To accommodate optical beam access into the crowded environment we mounted the mirror as close to the loaded gear tooth as possible, on the loading jigs fixture arm. Any movement experienced by the loaded tooth results in deflections of the mirror since the load arm insert and the gear tooth was in intimate contact throughout the test. The deflection of the laser beam by the reflecting surface of the mirror varied the amount of light that passed by the knife edge and was focused on the detector by collecting optics. As the mirror tilts, the optical beam path deflects by d at the knife edge according to the expression

$$d = l \tan(2\phi) \quad (1)$$

l is the distance to the knife edge from the vibrating mirror, and ϕ is the rotation of the sensing mirror. By positioning the knife edge to intercept a portion of the beam, the amount of light

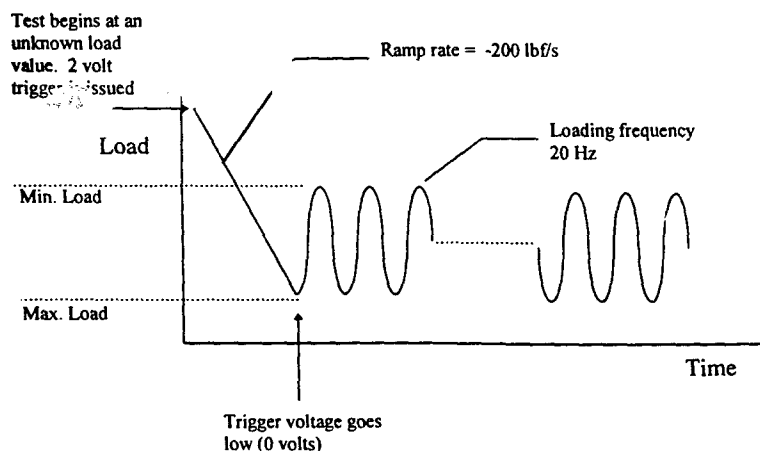


Figure 2. MTS loading profile

focused onto the detector will be modulated by the motion of the sensing mirror. For an collimated laser beam, operating in the TEM_{00} mode, the spatial variation of intensity has a radial Gaussian distribution given by

$$I(r) = \frac{2P_t}{\pi\omega^2} \exp\left(-\frac{2r^2}{\omega^2}\right) \quad (2)$$

where r is the distance from the beam center, w is the halfwidth of the beam (the points where the intensity drops to e^{-2} times that of the center) and P_t is the total power in the beam [3]. The voltage output of the photo diode will be proportional to the light power imaged onto the detector, defined by the unmasked portion of the beam that falls on the detector

$$P = \frac{2P_t}{\pi\omega^2} \iint \exp\left(-\frac{2r^2}{\omega^2}\right) r dr d\theta \quad (3)$$

with the limits of integration given as function of d .

Voltage data was collected at a rate of 500 samples per second and stored on a personal computer using PC based software and a 12 bit A/D card. Since the deflection due to crack growth/opening were seen to be much smaller than the elastic deflection of the gear tooth caused by cyclical loading, it was imperative that the entire dynamic range of A/D be utilized. Alignment of the optical beam was performed so that the laser beam was captured by the collecting optics and focused on to the active area of the photodiode throughout the entire displacement cycle. Next, the intensity of light was adjusted using a variable attenuator so that

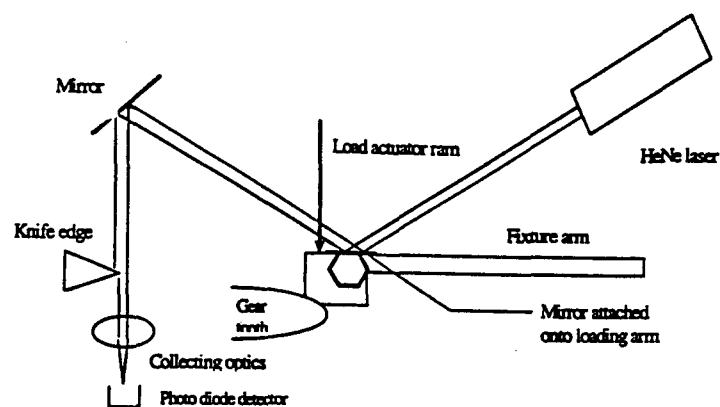


Figure 3. Knife edge detection set up used for optical detection of gear tooth deflection

the maximum light intensity did not saturate the photodiode device. After the fatigue loading ended, a static calibration curve was generated to relate deflection to voltage output by driving the ram into a known deflection position and recording the output voltage. Unfortunately the dynamic loading conditions produced deflections that differed substantially from the statically loaded deflections.

ACOUSTIC EMISSION MEASUREMENTS: Acoustic Emission (AE) is an elastic stress wave generated by the rapid release of energy within a material. Plastic deformation, crack initiation, and crack growth from fatigue or corrosion produce acoustic emission signals. The energy that is converted to AE signals comes from the material itself. As a result, this nondestructive technique is sensitive to initiation and propagation of defects. Several parameters are necessary to define an acoustic emission event or hit. Figure 4 illustrates the primary terms used to describe the signal from one AE event. The AE signal is monitored as the voltage response as a function of time, $V(t)$, from the transducer. The noise level refers to the background noise. Successful AE testing relies on the ability to detect the signals of interest above the background noise. Background noise problems range from negligible to severe, depending on the test conditions. For fatigue testing, mechanical noise sources include: test machine noise, flow noise from pumps and valves, and all types of frictional processes (e.g., guide fixtures, contact points, and pivot points). One of primary ways of excluding background noise is the use of a threshold. When the amplitude of an AE signal exceeds this voltage

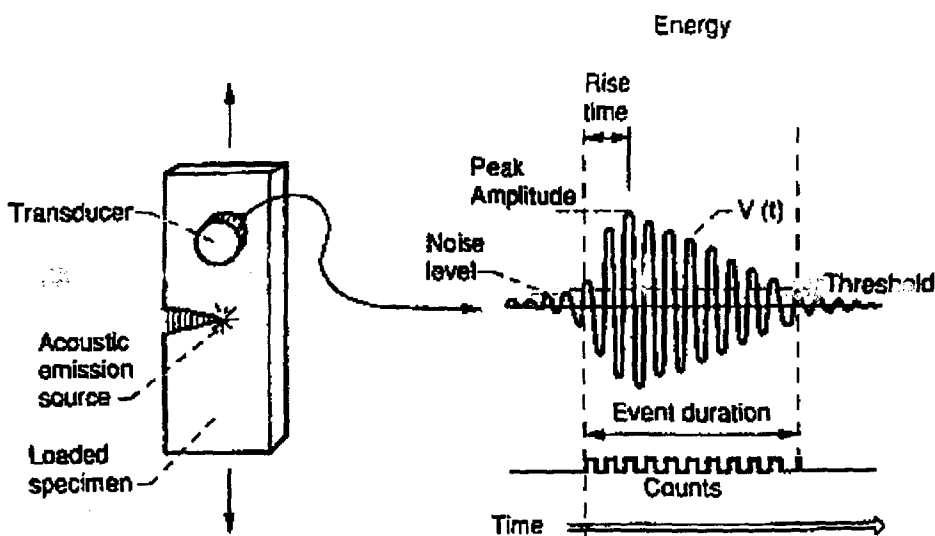


Figure 4. Definition of acoustic emission event parameters

threshold, an event or 'hit' is recognized and the event parameters are recorded. These specific signal parameters include: the peak (maximum) amplitude, the rise time, the signal duration, the signal counts, and the signal energy. The peak amplitude represents a measure of the signal strength and therefore governs the detectability of the event. The rise time is the time from the first threshold crossing to the signal peak. This parameter is useful for source discrimination and signal filtering. Duration is defined as the time from the first threshold crossing to the last and may be used for source discrimination. Counts (threshold crossing counts) are the number of times the AE signal crosses the threshold and gives a simple measure of the signal size. The signal energy is the calculated area under the rectified signal envelope and provides a combined view of peak amplitude and signal duration.

Acoustic emission data was collected during each fatigue test using a LOCAN-AT acoustic emission unit made by Physical Acoustics, Inc. Each gear was instrumented with a broadband (100-1000 kHz) acoustic emission transducer. The transducer was centered on a flat region of the gear just above the tooth being loaded. The transducer position was selected for protection of the transducer, location near the tooth being tested, and coupling of the transducer to a flat region of the gear. Calibration of the transducer response in this orientation was performed using the standard mechanical pencil lead break test on the test tooth. This calibration test produced an 80-84 dB amplitude response indicating strong coupling of the transducer to the gear and high sensitivity of any acoustic emission events from the tooth region. The acoustic emission (AE) system was synchronized with the start of the cyclic loading via a voltage trigger from the MTS control panel. Acoustic emission data was collected on a hit-driven basis, meaning that data was only collected when a signal threshold value was reached.

DATA ANALYSIS AND RESULTS: Figure 5 shows macrographs of two gears visually inspected after the cyclically fatigue testing was complete. Both gears were driven in the same manner and reached the same level of deflection before the loading cycle was halted. Notice that the gear on the right, made from VASCO-X2, does not show any significant cracking. In contrast, the gear on the left, made from AMS-6265, which shows a severe, 0.7 cm long, crack starting from the tooth root. The data sets from these two gear teeth were used in the ensuing data analysis.

In order to provide features that might be useful to a prognostic model, our approach was to examine changes within the data with respect to a dependent variable that relates back to the fatigue loading condition. A convenient and effective observable which provides a measure of the load experienced by the tooth was found to be given by

$$Accumulated\ load = \int_0^{cycles} PdN \quad (4)$$

For the sinusoidal driving function used in our experiment this parameter simplifies to the product of mean load multiplied by the number of cycles, $P_{mean}N$. The deflection data collected from the MTS sensor was processed by using a moving average filter to remove the 20 Hz cyclical variation that arose due to the elastic deflection response of the gear tooth to the cyclical

loading. This processed result was then subtracted from a base line average value established from the initial portion of the data record. This result provided a differential moving average deflection value as a function of accumulated load. The most revealing feature obtained from the acoustic emission data was the relationship between accumulated acoustic emission energy and the accumulated load parameter. This relationship is physically founded since we expected the strain energy released during crack tip advances to generate significant acoustic emission (AE). Unfortunately it was difficult to discriminate these AE events from the high background noise. The optical data was initially processed in a manner similar to the MTS deflection data. A high pass filter was applied to remove the 20 Hz response of the dynamic loading and the resulting signal was squared to provide a mean squared voltage value plotted against accumulated load. The results of these analyses for two different sets of gear data are compared in Figures 6 - 8.

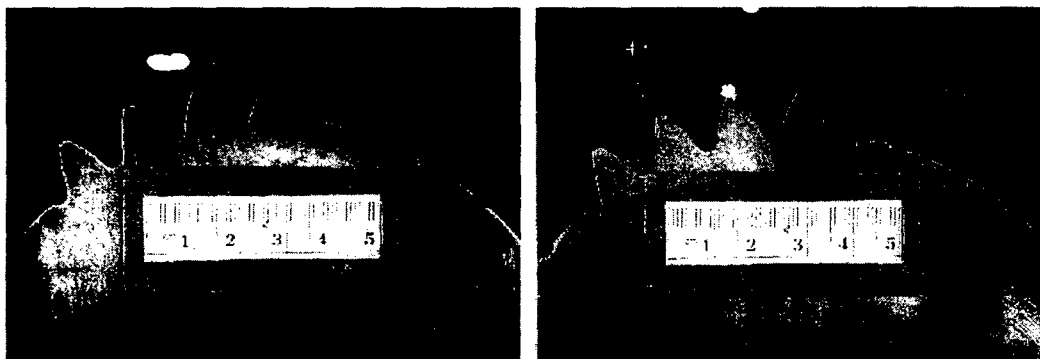


Figure 5. Macrographs of gear teeth after fatigue loading. The right image shows a gear made from AMS-6265, while the left image shows a gear made from VASCO-X2

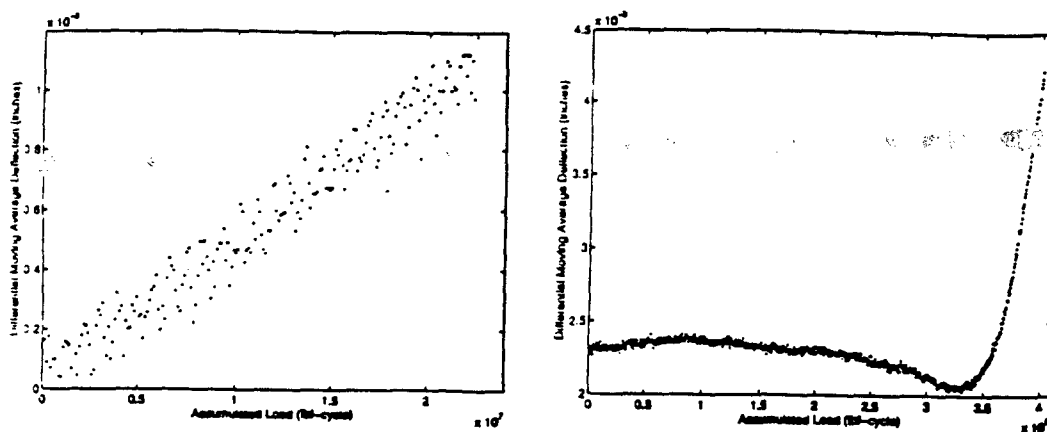


Figure 6. Comparison of differential moving average deflection calculated from AMS-6265 (right side) and VASCO-X2 (left side) gear data

In each of the respective figures, the analyzed data from the cracked, AMS-6265, is shown on the right hand side, while the left hand side shows the computed results from the VASCO-X2 gear data. Notice that the results for the AMS-6265 data all consistently indicate a dramatic deviation, from an initial trend, at an accumulated load value of ~ 3.4 lbf-cycle. The uncracked gear, VASCO-X2 does not indicate this behaviour. In the case of the AMS-6265 gear we believe that these departures from initial trend values occurred when the micromechanical mechanism of gear fatigue transitioned from crack initiation to crack growth/propagation. Closer inspection of the results for the AMS-6265 gear showed that the high rate of AE energy release predated the

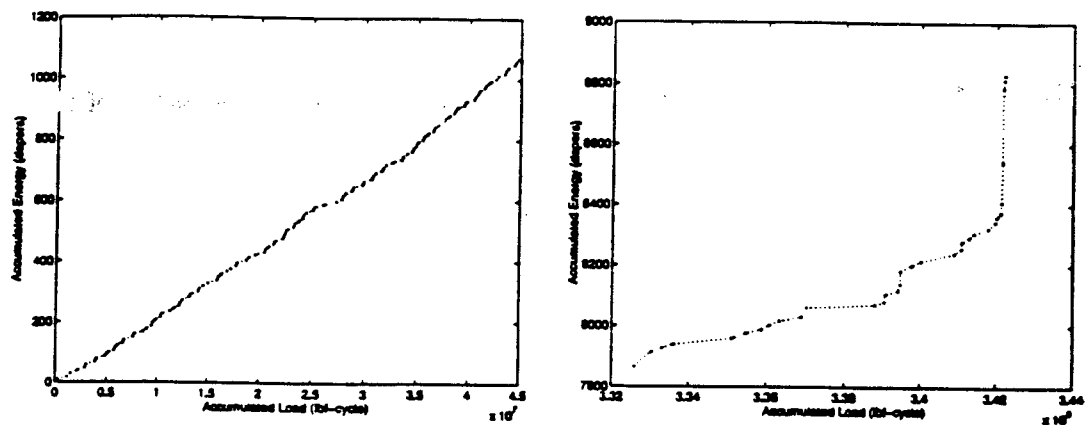


Figure 7. Comparison of accumulated acoustic emission energy calculated from AMS-6265 (right side) and VASCO-X2 (left side) gear data

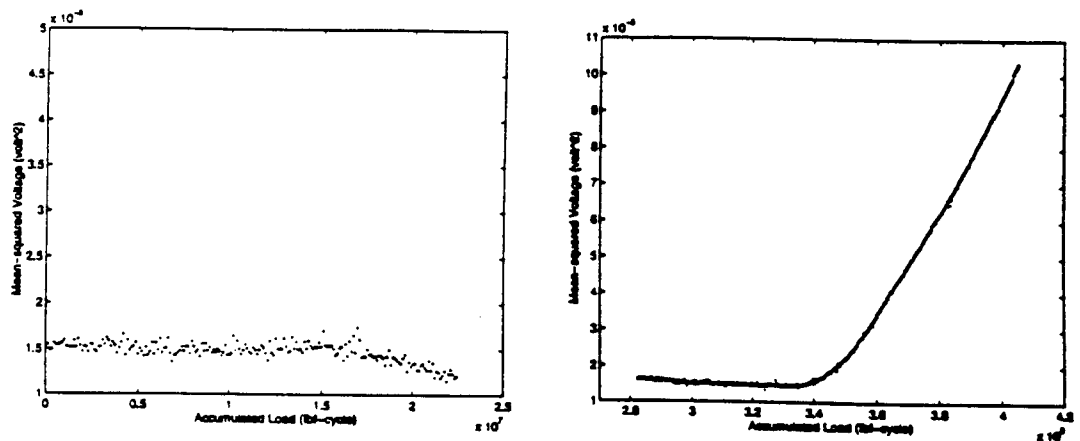


Figure 8. Comparison of mean squared voltage values calculated from photodiode response of AMS-6265 (right side) and VASCO-X2 (left side) gear data

moving average deflection feature by ~ 2500 cycles, or 3 % of the total number of cycles. The results from the optical data analysis were also consistent with the moving average deflection feature. However the high sampling rate of the optical data provided an opportunity to investigate more sophisticated analysis procedures.

SIGNAL PROCESSING BY CYCLOSTATIONARITY: The periodic nature of the loading suggested application of cyclostationary signal processing techniques for studying the frequency spectrum of the observed deflection signal. These techniques have been successfully applied to various problems in communication systems. We selected the optical photodiode voltage measurements for our analysis due to the higher sampling rate used, which allows higher harmonics to be studied. Cyclostationary processing should provide a better estimate of the harmonic content of the observed signal which gives an indication of abnormal mechanical activity. In this section we present some preliminary results of cyclostationary processing of the observed signal.

We use the definition in [5] of the cyclic spectral-correlation density (SCD) of a signal $x(t)$ is defined as

$$S_x^\alpha(f) = \lim_{B \rightarrow 0} \frac{1}{B} \langle [h_B^f(t) * x(t) \exp(j\pi\alpha t)] [h_B^f(t) * x(t) \exp(-j\pi\alpha t)]^* \rangle \quad (5)$$

where $h_B^f(t)$ is a one-sided narrowband filter with center frequency f and bandwidth B , * denotes

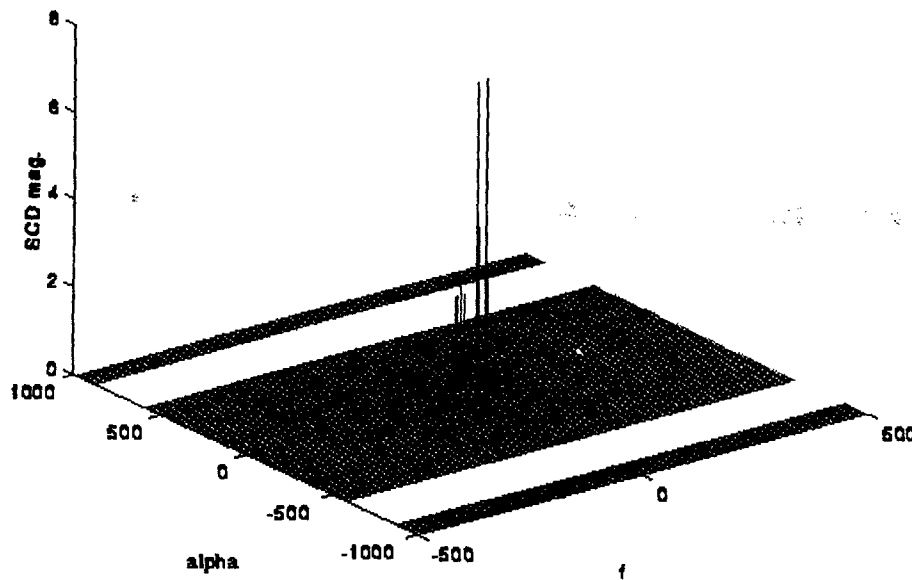


Figure 9. SCD magnitude of the photodiode voltage signal prior to crack propagation (70000-75000 cycles)

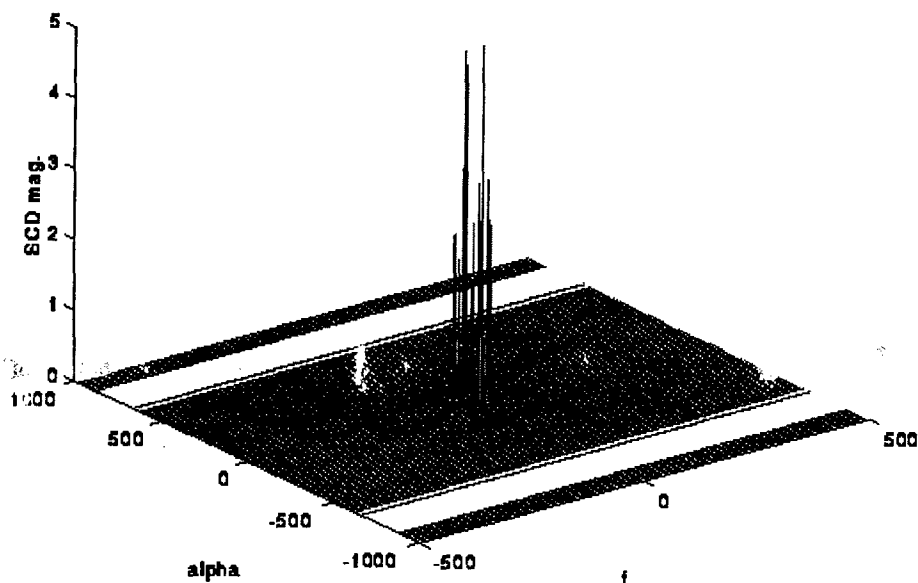


Figure 10. SCD magnitude of the photodiode voltage signal during crack propagation (75000-84000 cycles)

the convolution operator, the superscript $*$ indicates the conjugation operation, and $\langle \rangle$ indicates the time-average operation. The above operation is performed for various values of α to obtain the entire SCD. We have shown in Figures 9 and 10 the magnitude of the SCD of the laser photodiode voltage signal during the last part of the run which resulted in a cracked tooth. The two line spectra clearly indicate a change in the nature of the signal. In particular, there are more spectral lines in Figure 10 than in Figure 9 but magnitude of the lines in Figure 10 is smaller than the lines Figure 9. This indicates that the fatigue in the tooth is observable in the spectral content of the deflection signal. This fact is corroborated by the presence of a crack during the visual inspection of the gear after the completion of the test and by other signal processing analysis described above.

CONCLUSIONS: We have described an experiment where multisensor data was collected during gear tooth fatigue studies. Although the number of data sets was not large, our analysis extracted several features which could be useful in a failure prediction model. These features were shown to be in agreement with the observed fatigue induced crack damage. We have also employed new techniques specifically designed for cyclostationary systems, such as rotating machinery. Having shown the viability of this approach, we believe that further investigation into to determine whether this approach can be utilized for predicting remaining useful life of machinery is warranted.

ACKNOWLEDGMENTS: The authors would like to thank Guillermo Astete for assisting in data collection and Dr. Steve Schell of Penn State's Electrical Engineering Department for providing the Matlab routines for the cyclic spectral analysis discussed in this paper.

REFERENCES:

- [1] Barkov, A. and Barkova, N. "Condition assessment and life prediction of rolling element bearings - Part1," *Sound and Vibration*, June 1995.
- [2] Hansen, R.J., Hall, D.L., and Kurtz, S.K. "A new approach to the challenge of machinery prognostics," *Transactions of the ASME*, **117**, pp. 320-325, April 1995.
- [3] Lemanski, A.J., and Rose, H.J. "Evaluation of advanced gear materials for gear boxes and transmission," Boeing Technical Report, No. D210-10345-1, 1971.
- [4] Collier, R.J., Burckhardt, and Lin, L.H. *Optical Holography*, Academic Press, Inc., NY, NY, 1971.
- [5] Scott, I.G. *Basic Acoustic Emission*, Gordon and Breach Science Publishers, NY, NY, 1991.
- [6] Gardner, Exploitation of spectral redundancy in cyclostationary signals, *IEEE Signal Processing Magazine*, pp. 14-36, April 1991.